Biological response and cell death signaling pathways modulated by tetrahydroisoquinoline-based aldoximes in human cells

Antonio Zandona, Josip Madunić, Katarina Miš, Nikola Maraković, Pierre Dubois-Geoffroy, Marco Cavaco, Petra Mišetić, Jasna Padovan, Miguel Castanho, Ludovic Jean, et al.

Biological response and cell death signaling pathways modulated by tetrahydroisoquinoline-based aldoximes in human cells

Antonio Zandona[1], Josip Madunić[1], Katarina Miš[2], Nikola Maraković[1], Pierre Dubois-Geoffroy[3], Marco Cavaco[4], Petra Mišetić[5], Jasna Padovan[5], Miguel Castanho[4], Ludovic Jean[6], Pierre-Yves Renard[3], Sergej Pirkmajer[2], Vera Neves[4], Maja Katalinić[1,*]

[1]Institute for Medical Research and Occupational Health, POB 291, HR-10001 Zagreb, Croatia; azandona@imi.hr, jmadunic@imi.hr, nmarakovic@imi.hr, mkatalinic@imi.hr
[2]Institute of Pathophysiology, Faculty of Medicine, University of Ljubljana, Ljubljana, Slovenia; katarina.mis@mf.uni-lj.si, sergej.pirkmajer@mf.uni-lj.si
[3]Normandie Univ, UNIROUEN, INSA Rouen, CNRS, COBRA (UMR 6014), 76000 Rouen, France; pierre.dubois-geoffroy@univ-rouen.fr, pierre-yves.renard@univ-rouen.fr
[4]Institute of Molecular Medicine, Faculty of Medicine, University of Lisbon, Lisbon, Portugal; mcavaco@medicina.ulisboa.pt, macastanho@medicina.ulisboa.pt, veraneves@medicina.ulisboa.pt
[5]Selvita Ltd., 10001 Zagreb, Croatia; Petra.Misetic@selvita.com, Jasna.Padovan@selvita.com
[6]Université Paris Cité, CNRS, INSERM, CiTCoM (UMR 8038), F-75006, Paris, France; ludovic.jean1@parisdescartes.fr
*****Correspondence: mkatalinic@imi.hr

ORCID:
Antonio Zandona, 0000-0002-3937-3520
Josip Madunić, 0000-0003-4724-9236
Katarina Miš, 0000-0002-1726-2686
Nikola Maraković, 0000-0002-1709-6390
Pierre Dubois-Geoffroy, 0000-0002-0770-855X
Marco Cavaco, 0000-0002-0938-9038
Petra Mišetić, 0000-0002-2275-2794
Jasna Padovan, 0000-0001-9829-6070
Miguel Castanho, 0000-0001-7891-7562
Ludovic Jean, 0000-0002-1745-4952
Pierre-Yves Renard, 0000-0001-9094-9778
Sergej Pirkmajer, 0000-0003-1459-6936
Vera Neves, 0000-0002-2989-7208
Maja Katalinić, 0000-0001-7043-4291

Abstract:
The uncharged 3-hydroxy-2-pyridine aldoximes with protonatable tertiary amines are studied as antidotes in toxic organophosphates (OP) poisoning. Due to some specific structural features they have, we hypothesize that these compounds could exert diverse biological activity beyond their main scope of application. To examine this further, we performed an extensive cell-based assessment to determine their effects on human cells and possible mechanism of action. As our results indicated, in the concentration range up to 800 μM, aldoxime having piperidine moiety did not induce significant toxicity, while those with tetrahydroisoquinoline moiety stimulated mitochondria-mediated activation of the intrinsic apoptosis pathway through ERK1/2 and p38-MAPK signaling and subsequent activation of initiator caspase 9 and executive caspase 3 accompanied with DNA damage. Mitochondria and fatty acid metabolism were also likely targets of 3-hydroxy-2-pyridine aldoximes, due to increased phosphorylation of acetyl-CoA carboxylase. *In silico* analysis predicted kinases as their most probable target class, while pharmacophores modeling additionaly predicted the inhibition of a cytochrome P450cam, as well. Overall, observed biological activity of aldoximes with tetrahydroisoquinoline moiety could be indicative for future design of compounds either in a negative context in OP antidotes design, or in a positive one for design of compounds for the treatment of other conditions and diseases, such as cancer.

Keywords: antidotes; oximes; apoptosis; pharmacophore; cell viability

Statements and declarations

Funding: This study was funded by the Croatian Science Foundation (UIP-2017-05-7260 to M.K.), Slovenian Research Agency (J3-3065 to S.P. and J3-2523, P3-0043 and J7-3153 to S.P. and K.M), Croatian-Slovenian Bilateral grant 2020-2021 (BI-HR/20-21-041). Part of this work was supported through the EMBO short term fellowship STF-8731 to A. Zandona in M. Castanho lab (Lisabon, Portugal) and by the Fundação para a Ciência e Tecnologia" (FCT, Portugal) (grants PTDC/BTM-MAT/2472/2021 and PD/BD/128281/2017). This work has also been partially supported by University of Rouen Normandy, the Centre National de la Recherche Scientifique (CNRS), INSA Rouen Normandy, European Regional Development Fund (ERDF), Labex SynOrg (ANR-11-LABX-0029), Carnot Institute I2C, the graduate school for research XL-Chem (ANR-18-EURE-0020 XL CHEM), and by Region Normandie.

Acknowledgments: We thank Prof Nino Sinčić and Dr Bojana Žegura for facilitating certain measurements at the School of Medicine, University of Zagreb, Croatia and at the National Institute of Biology, Ljubljana, Slovenia, respectively. We thank Dr Zrinka Kovarik, Institute for medical Research and Occupational Health, Zagreb, Croatia for the use of Biovia Discovery Studio Client software (RRID:SCR_015651, Dassault Systèmes, Vélizy-Villacoublay, France) provided through Croatian Science Foundation projects (grant numbers HrZZ-IP-2013-11-4307 and HrZZ-IP-2018-01-7683 to Z. Kovarik). The authors thank Région Normandie and French DoD procurement agency for PhD fellowship to P. D-G.

Institutional Review Board Statement: All studies on the primary human skeletal muscle cells reported here were conducted at the Institute of Pathophysiology, Faculty of Medicine, University of Ljubljana, Ljubljana, Slovenia. The use of human skeletal muscle cells (HSMC) was approved by the Republic of Slovenia Medical Ethics Committee (#71/05/12 and #0120-698/2017/4). The manuscript does not contain clinical studies or patient data.

Conflicts of Interest: The authors have no competing interests to declare that are relevant to the content of this article.

Data availability: The datasets generated during and/or analysed during the current study are available from the corresponding author on reasonable request.

Introduction

This paper presents continuation of our previous research describing a wider biological potential of compounds known as oximes, specifically designed as acetylcholinesterase-based ligands (Zandona et al. 2021, 2022). Namely, oximes, having the oxime functional group (NOH), are designed as reactivators/antidotes of acetylcholinesterase (AChE, EC 3.1.1.7) inhibited by highly toxic organophosphorus (OP) pesticides or nerve warfare agents (Worek et al. 2020). Our studies on pyridinium oximes as one of the antidotes scaffolds, have shown that due to the specific structural features (like presence of one or more aromatic rings, oxime and alcohol groups, nitrogen and chlorine atoms), they could exhibit other biological activities, like inducing oxidative stress, regulated cell death apoptosis, or interact with cholinergic receptors (Soukup et al. 2011; Muckova et al. 2019; Zandona et al. 2021, 2022; Gašo Sokač et al. 2022). Such results put forward oximes as interesting scaffolds for drug design outside their involvement in the field of antidotes development.

Here, we extended our research to the uncharged 3-hydroxy-2-pyridine aldoximes, described recently as potential reactivators of human synaptic AChE (Zorbaz et al. 2018). These oximes were specifically designed to span the AChE active site achieved by connecting pyridine aldoxime through an aliphatic linker to simple protonatable tertiary amines (morpholine, piperidine), than fused with dimethoxybenzene (dimethoxytetrahydroisoquinoline) and substituted with N,N-dimethylaniline (1-[4-(N,N-dimethylamino)phenyl]-1,2,3,4-tetrahydroisoquinoline (Fig. 1).

Looking in the aspect of the chemical structure, 3-hydroxy-2-pyridine aldoximes carry motif/s of already reported biologically activity (in example hydroisoquinoline moiety (Saitoh et al. 2006; Kotake et al. 2007; Garcia et al. 2010; Truax et al. 2013; Zorbaz et al. 2018; Zandona et al. 2020)), which makes them, in the start, their structural analogues worth further investigation. For instance, compounds with the hydroisoquinoline moiety have been investigated as CXCR4 antagonists (Truax et al. 2013).

In this study, we aimed to screen several uncharged 3-hydroxy-2-pyridine aldoximes (Fig. 1) by determining their effects on the cell level, and the mechanism behind their action. Effects were evaluated on 6 different cell types representing the liver, kidney, neurons and muscles (4 cell lines, two primary cell cultures) for better understanding of aldoximes action and overall analysis of the obtained results. These cells represent well established major organ models and are selected due to the possibility of being affected by tested compounds or included in their metabolism and/or excretion according to the known literature data (Bouma et al. 1989; Ryan et al. 1994; Thomas and Smart 2005; Xie et al. 2010; Gunness et al. 2010; Kovalevich and Langford 2013; Aas et al. 2013; Abdelmoez et al. 2020). The results will reveal the potential link between aldoximes' protonatable moiety and their cellular effects and help in clarifying the potential of 3-hydroxy-2-pyridine aldoximes to be further developed as new AChE-based antidotes or as drugs for the treatment of other conditions like cell proliferating malignancies.

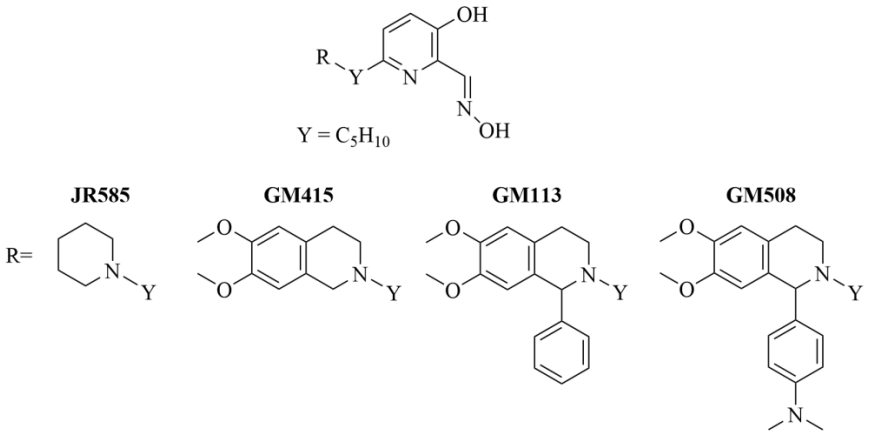

Fig. 1 Structure of 3-hydroxy-2-pyridine aldoximes tested in this study

Materials and Methods

Aldoximes and cells

All tested aldoximes were synthesized previously by Prof Pierre-Yves Renard's group at Normandie University (UNIROUEN, INSA Rouen, CNRS, Rouen, France) (Zorbaz et al. 2018) (presented in Fig. 1). Aldoximes JR585, GM415, GM113 and GM508 were dissolved in DMSO as 100 mM stock solutions before use. Further dilutions were made in unsupplemented cell medium before the experiment.

Human neuroblastoma SH-SY5Y (ECACC 94030304, RRID:CVCL_0019), human Caucasian hepatocyte carcinoma HepG2 (ECACC 85011430, RRID:CVCL_0027), human embryonic kidney HEK293 (ECACC 85120602, RRID:CVCL_0045), and human adult kidney HK-2 (ATCC® CRL-2190™, RRID:CVCL_0302) cells were obtained from certified cell-banks. Satellite cells were isolated from human skeletal muscle tissue routinely discarded at standard orthopedic surgery from donors free of neuromuscular disease and were grown and differentiated to human primary myoblasts and myotubes as described earlier (Dolinar et al. 2018; Pirkmajer et al. 2020). Donors of skeletal muscle tissue signed a written consent, and the use of human skeletal muscle cells (HSMC) was approved by the Republic of Slovenia Medical Ethics Committee (#71/05/12 and #0120-698/2017/4). All studies on the primary human skeletal muscle cells reported here were conducted at the Institute of Pathophysiology, Faculty of Medicine, University of Ljubljana, Ljubljana, Slovenia, using three different donors. SH-SY5Y cells were grown in DMEM F12 medium (Sigma–Aldrich, Steinheim, Germany) supplemented with 15 % (*v/v*) fetal bovine serum (FBS) (Sigma-Aldrich, Steinheim, Germany), 2 mM glutamine (Sigma-Aldrich, Steinheim, Germany), 1 % (*v/v*) Penicillin/streptomycin (PenStrep, Sigma-Aldrich, Steinheim, Germany) and 1 % (*v/v*) non-essential amino acids (NEAA, Sigma-Aldrich, Steinheim, Germany). HEK293 and HepG2 cells were grown in EMEM medium (Sigma-Aldrich, Steinheim, Germany) supplemented with 10 % (*v/v*) FBS (Sigma-Aldrich, Steinheim, Germany), 2 mM glutamine (Sigma-Aldrich, Steinheim, Germany), 1 % (*v/v*) PenStrep (Sigma-Aldrich, Steinheim, Germany) and 1 % (*v/v*) NEAA (Sigma-Aldrich, Steinheim, Germany). HK-2 cells were grown in DMEM:F12 medium (1 g/L glucose, Gibco, Paisley, UK) supplemented with 10 % (*v/v*) FBS (Gibco, Paisley, UK), 1 % (*v/v*) PenStrep (Gibco, Paisley, UK) and 0.3 % (*v/v*) Fungizone (Invitrogen, UK). Myoblasts were grown in advanced minimal essential medium (advMEM; ThermoFisher, USA), supplemented with 10 % (*v/v*) FBS (ThermoFisher, USA), 0.3 % (*v/v*) Fungizone (ThermoFisher, USA), 0.15 % (*v/v*) Gentamicin (ThermoFisher, USA). Myoblasts were differentiated into myotubes according to a standard procedure (Dolinar et al. 2018; Pirkmajer et al. 2020), in advMEM medium supplemented with 2 % (*v/v*) FBS, 0.3 % (*v/v*) Fungizone and 0.15 % (*v/v*) Gentamicin.
All cells were maintained at 37 °C in 5 % CO_2-enriched air at saturation humidity, the medium was changed every two to three days, and passages were performed according to the standard protocol (ECACC 2017).
Phosphate-buffered saline (PBS, pH 7.4) was prepared according to a standard recipe (Dulbecco and Vogt 1954)and used for washing the cells when needed in the assays.
In every method used, the blank (only compound) was tested due to the possibility of interference. In all methods, the compound was washed with buffer before the addition of the dye, except for membrane integrity assay, which was considered.

Cytotoxicity of aldoximes

The cytotoxic profile of tested aldoximes was determined by measuring the succinate dehydrogenase mitochondrial activity in exposed cells (Mosmann 1983). For this purpose, we used the commercially available MTS detection reagent assay (CellTiter 96® AQueous One Solution Cell Proliferation Assay, Promega, Madison, WI, USA). The procedure followed a previously described protocol (Zandona et al. 2021), and the effect was determined after 1, 4, and 24 hours exposure to aldoximes. The total percentage of DMSO in the assay was 0.8 % and did not influence cell viability. Staurosporine was used as a positive control, and HI-6 as negative control. This data for staurosporine and HI-6 were reported previously in another study (Zandona et al. 2021) so it is only cited here in the corresponding result table. Data were evaluated from at least three independent experiments (performed in duplicate or triplicate) and presented as a percentage of the observed inhibition of cell viability compared to control untreated cells. From experimental data, IC_{50} values (concentration of aldoxime that kills 50 % of cells) were determined by a nonlinear fit equation predefined in Prism software (RRID:SCR_002798, GraphPad Software, San Diego, USA). Also, from these data aldoxime concentrations corresponding to Lowest Observed Adverse Effect Level or LOAEL concentrations (Timbrell 2000) were determined as concentration that killed ≈ 20-25 % of cells in 24 hours.
The same MTS method was used to evaluate a potential toxic synergistic effect in SH-SY5Y cells exposed to a combination of two aldoximes at LOAEL concentrations (Timbrell 2000).

Cell membrane integrity

Cell membrane integrity was determined by measuring the release of the intracellular lactate dehydrogenase (LDH) from cells with a damaged membrane into the medium (Decker and Lohmann-Matthes 1988). The procedure followed a previously described protocol (Zandona et al. 2021). Triton X-100 at a final concentration of 0.18 % (*v/v*) (9 % in water stock; Sigma-Aldrich, Steinheim, Germany) was used as a positive control to determine maximal LDH release. Data were evaluated from at least two or three independent experiments (performed in duplicate or triplicate) using Prism software and presented as a percentage of LDH release compared to the determined maximal LDH release. Calculations were done according to the predefined equation from CytoTox-ONE™ Homogeneous Membrane Integrity Assay kit protocol.

Oxidative status of cells

Induction of reactive oxygen species (ROS) by aldoximes was determined using a cell-permeable reagent 2',7'–dichlorofluorescein diacetate dye (DCFDA, Sigma-Aldrich, Steinheim, Germany). The procedure followed a previously described protocol (Zandona et al. 2021). Hydrogen peroxide (H_2O_2, Sigma-Aldrich, Steinheim, Germany), 100 µM final concentration, was used as a positive control. Data was evaluated from at least two or three independent experiments (performed in duplicate or triplicate) using Prism software and presented as a normalized signal to the untreated cells, according to the manufacturer's calculation protocol.

Mitochondrial membrane potential ($\Delta\Psi_m$) changes

Mitochondrial membrane potential ($\Delta\Psi_m$) was determined using a cell-permeable potential-sensitive cationic dye tetramethylrhodamine ethyl ester perchlorate (TMRE, Cell Signaling Technology Europe, Leiden, The Netherlands). The procedure followed a previously described protocol (Zandona et al. 2021). A concentration of 50 µM carbonyl cyanide 3-chlorophenylhydrazone (CCCP, Cell Signaling Technology Europe, Leiden, The Netherlands) was used as a positive control. Data was evaluated from at least three independent experiments (performed in duplicate) using Prism software and presented as a normalized signal to the untreated cells, according to the manufacturer's calculation protocol.

Induction of apoptosis

Aldoxime-mediated induction of apoptosis was analyzed by detecting the translocation of phosphatidylserine (PS) to the cell surface using an Annexin V probe and following loss of membrane integrity using 7-aminoactinomycin D (7-AAD) dye. For this purpose, we used predefined Muse® Annexin V & Dead Cell Assay (Merck KGaA, Darmstadt, Germany), which distinguishes between four populations of cells as follows: non-apoptotic, early apoptotic, late stage apoptotic and dead cells. The procedure followed a previously described protocol (Zandona et al. 2021). Paraformaldehyde (PFA, Sigma-Aldrich, Steinheim, Germany), 0.08 % final, was used as a positive control. Data was evaluated by Muse™ and Prism software, and presented as a percentage of apoptotic cells compared to the control.

Caspase activity measurement

Crucial caspases (cysteine-aspartic proteases); caspase 3, caspase 8, and caspase 9, were simultaneously analyzed in SH-SY5Y cells, using specific substrate and fluorogenic indicators from Caspase-3, Caspase-8, and Caspase-9 Multiplex Activity Assay Kit (Abcam, Cambridge, UK). The procedure followed a previously described protocol (Zandona et al. 2021). A total of 3 µM staurosporine (Sigma-Aldrich, Steinheim, Germany) was used as positive control. This data for staurosporine was published previously with another study (Zandona et al. 2021)so it is only cited here in the corresponding result table. Data was evaluated from at least three independent experiments (performed in duplicate or triplicate) using Prism software, according to the manufacturer's assay kit calculation protocol.

DNA damage

In order to quantify DNA damage, we simultaneously measured levels of activated kinase ATM and phosphorylated histone H2A.X in the control and aldoxime-treated cells using predefined kit (Muse Multi-Color DNA Damage Kit, Luminex, Poland) for flow cytometer Muse™ Cell Analyzer (Luminex, Poland). Phosphorylation of these two proteins points to the induction of DNA damage response through ATM-dependent signaling pathway and indicates the occurrence of DNA double-stranded breaks in cells. Analysis was performed according to manufacturer's recommendations. Briefly, SH-SY5Y cells were seeded in 12-well plates at a density of 100,000 cells/well. Upon reaching 90 % confluence (~3 days), cells were exposed to LOAEL concentrations of aldoximes for 4 hours. After treatment, cells were washed with PBS and detached using 0.25 % Trypsin/EDTA solution (Sigma-Aldrich, Steinheim, Germany). Further action of trypsin was blocked using 500 µL of matching complete cell media (supplemented with 5 % FBS), and cell suspension was transferred to Eppendorf tubes for centrifugation at 300xg for 5 min. Pellet was resuspended with assay buffer and cells were afterwards fixed for 10 min on ice, followed by washing step in assay buffer. After fixation and another centrifugation, cells were permeabilized (10 min on ice) and washed again. Next, 100 000 cells were resuspended in 90 µL of assay buffer and 10 µL of PE/PECy5-conjugated antibody cocktail (5 µL of anti-phospho-ATM (Ser1981) and 5 µL of anti-phospho-Histone H2A.X (Ser139)) was added to each sample. Following 30 min of immunostaining at RT in dark, samples were washed and analyzed on flow cytometer. Treatment with 10 µM etoposide (Sigma-Aldrich, Steinheim, Germany) for 24 hours was used as a positive control. Each analysis was performed three times, in duplicates. Results were analyzed by Muse™ and Prism software and presented as a relative percentage of total DNA damage compared to control.

P-glycoprotein substrate assessment, in vitro BBB translocation and BBB integrity, and in silico physicochemical properties prediction

P-glycoprotein (P-gp) substrate assessment using the Madin-Darby canine kidney epithelial cell line with the overexpressed human MDR1 gene (MDCKII-MDR1, RRID:CVCL_S586), purchased from Solvo Biotechnology (SB-MDCKII-MDR1, Szeged, Hungary) was done at the Selvita Ltd., Zagreb, according to the procedure and the calculation previously described (Polli et al. 2001; Zorbaz et al. 2020; Zandona et al. 2021).
Human cerebral microvascular endothelium cells (HBEC-5i, ATCC CRL-3245, RRID:CVCL_4D10) were used for *in vitro* BBB translocation and integrity assays according to previously described protocol (Cavaco et al. 2020b, a, 2021).
The following physicochemical properties of compounds were estimated *in silico* with SwissADME (RRID:SCR_012880) (Daina et al. 2017): calculated logarithm of the octanol-water partition coefficient (clogP), topological polar surface area (TPSA), number of hydrogen-bond donors (HBD) and acceptors (HBA), number of rotatable bonds (RB). The obtained results for the tested aldoximes were compared to the recommendations for physicochemical properties of a successful central nervous system drug(Pajouhesh and Lenz 2005; Desai et al. 2012; Matsson and Kihlberg 2017).

Signaling pathway targets analysis by Western blot

After treatment with LOAEL concentrations, at the end of the experiment, cells were prepared as previously described (Pirkmajer et al. 2020). Proteins were resolved with SDS-PAGE (4-12 % polyacrylamide gels) and transferred to the PVDF membrane with wet electrotransfer. After blocking, membranes were incubated with a primary antibody (Table 1) in the primary antibody buffer (20 mM Tris, 150 mM NaCl, pH 7.5, 0.1 % (*w/v*) BSA and 0.1% (*w/v*) sodium azide) overnight at 4 °C and then with the secondary antibody Goat Anti-Rabbit IgG (H+L)-HRP Conjugate (Bio-Rad Laboratories, USA) in TBST buffer with 5 % (*w/v*) dry milk for 1 hour at room temperature. Membranes were incubated with ECL reagent (Pierce, Thermo Scientific, USA) or Immobilon Crescendo HRP substrate (Millipore, USA) and then immunolabeled proteins (chemiluminescent signal) were visualized and documented with Fusion FX System, Vilber, (dark box with high resolution camera; https://www.vilber.com/fusion-fx/) and densitometrically analyzed with Quantity One 1-D Analysis Software (Bio-Rad). Intensities of individual bands were expressed in arbitrary units relative to the total intensity of all the bands. Results are presented means ± SD (n = 5–9), sample vs. basal (B) by unpaired one-way ANOVA, Dunnett's test.

Table 1. Primary antibodies (Cell Signaling Technology Inc, USA) used for the western blot analysis.

Antibody	RRID	Cat. No.	Host	Type	Dilution
Anti p-ERK (Thr202/Tyr204)	AB_2315112	#4370	Rabbit	Monoclonal	1:2000
Anti pNFκB p65 (Ser536)	AB_331284	#3033	Rabbit	Monoclonal	1:2000
Anti p-p38 MAPK (Thr180/Tyr182)	AB_2139682	#4511	Rabbit	Monoclonal	1:1000
Anti p-STAT3 (Tyr705)	AB_2491009	#9145	Rabbit	Monoclonal	1:1000
Anti p-ACC (Ser79)	AB_330337	#3661	Rabbit	Polyclonal	1:1000
Anti p-AMPKα (Thr172)	AB_331250	#2535	Rabbit	Monoclonal	1:1000

Pharmacophore modeling and in silico prediction of cytochrome P450 inhibition

The pharmacophore models were generated using the Common feature pharmacophore generation protocol implemented in Discovery Studio software (RRID:SCR_015651, Dassault Systèmes, Vélizy-Villacoublay, France) as previously described (Zandona et al. 2021). Search 3D Database protocol using Catalyst was used to identify ligands in the database - DruglikeDiverse (5384 compounds), MiniMaybridge (2000 compounds), Sample (81 compounds), and scPDB (5465 compounds) that best maps to the generated pharmacophore and align the returned ligands to the query. The returned ligands were ranked in terms of FitValue – a measure of how well the ligand fits the pharmacophore. The online platform SwissADME (RRID:SCR_012880) was used to predict *in silico* if the selected antidotes inhibited relevant cytochrome P450 (CYPs) enzymes (Daina et al. 2017) and SwissTargetPrediction (RRID:SCR_012880) to estimate the most probable macromolecular targets of a small molecule, assumed as bioactive (Daina et al. 2019).

Statistics

Results are presented as mean with standard error if not stated otherwise. One-way ANOVA followed by Dunnett's multiple comparisons test was performed to test for differences among groups. Statistical analyses were done using

Prism software (RRID:SCR_002798, GraphPad Software, San Diego, USA). Statistical significance is shown as follows: &p < 0.05; #p < 0.01; $p < 0.001; *p < 0.0001.

Results

Tetrahydroisoquinoline moiety provoked cytotoxic effects

The cytotoxic effect of 3-hydroxy-2-pyridine aldoximes was here thoroughly evaluated on SH-SY5Y, HEK293, HK-2, and HepG2 cells and on primary myoblasts and myotubes after 24-hour exposure period. Effect on SH-SY5Y in 24-hour exposure experiments were reported previously (Zorbaz et al. 2018) (except GM113) and are presented here for comparison. The aldoximes' concentration range was selected to correspond to therapeutically relevant concentrations and ones used to assess their antidotal properties *in vitro* (Calas et al. 2017; Zorbaz et al. 2018; Sit et al. 2018; Taylor et al. 2019; Zandona et al. 2020). The results obtained, expressed as IC_{50} values, are presented in Table 2. According to the results, we observed that aldoxime JR585, bearing a protonable piperidine group as AChE peripheral site ligand, showed no significant toxicity on any of the cell types in the studied concentration range up to 800 µM and 24-hour time frame tested. On the contrary, three out of four aldoximes, GM415, GM113 and GM508, were toxic to most cells in concentration from 8-300 µM. We thus decided to more precisely assess these three aldoximes in order to understand which moiety is responsible for the observed effects. As a first evidence, it can be noted that the presence of additional phenyl (GM113) or 4-(dimethylamino)phenyl (GM508) moieties increased toxicity compared to GM415 depending on the cell line. As expected, oxime HI-6 used as a reference (one of the three oximes approved for medical use (Worek and Thiermann 2013)) showed no toxic effect, while the positive control, staurosporine, had pronounced toxicity (Zandona et al. 2021). Based on these results of 24-hour cytotoxicity screening, we selected GM415, GM113 and GM508 aldoximes for further analysis.

Table 2 The cytotoxicity of tested 3-hydroxy-2-pyridine aldoximes evaluated by MTS assay after 24-hour cell exposure expressed as IC_{50} values (µM)

Compound	SH-SY5Y	Myoblasts	Myotubes	HepG2	HEK293	HK-2
JR585	513 ± 6[a]	≥ 800	≥ 800	533 ± 2	490 ± 1	≥ 800
GM415	154 ± 1[a]	8 ± 1	309 ± 1	152 ± 2	126 ± 2	299 ± 3
GM113	44 ± 1	≥ 300	≥ 300	27 ± 1	13 ± 1	≥ 300
GM508	47 ± 1[a]	41 ± 1	93 ± 1	23 ± 1	49 ± 1	86 ±1
HI-6	≥ 800[a]	≥ 500	≥ 800	≥ 800	≥ 800	≥ 800
Staurosporine[b]	0.12 ± 0.01	0.15 ± 0.02	0.13 ± 0.001	> 2	0.02 ± 0.001	≤ 0.015

[a] from (Zorbaz et al. 2020), and [b] (Zandona et al. 2021)

Next, we evaluated 3-hydroxy-2-pyridine aldoximes' time dependent toxicity at 1- and 4-hour. According to the results shown in Table 3, the toxic effect of aldoximes was time-dependent in all cell types compared to the results of 24-hour cell exposure (see Table 2). Namely, toxic effects were not observed within 1-4 hours on most cell lines tested, but increased in time after, and resulted in cell death observed at 24-hour time point (see Table 2). An exception was observed only for SH-SY5Y exposed to GM508, and for HEK293 cells exposed to all three aldoximes.

Table 3 Cytotoxicity of selected 3-hydroxy-2-pyridine aldoximes evaluated by MTS assay after 1- and 4-hour cell exposure expressed as IC_{50} values (µM)

Aldoxime	Exposure time (h)	SH-SY5Y	Myoblasts	Myotubes	HepG2	HEK293	HK-2
GM415	1	≥ 500	≥ 500	≥ 500	≥ 500	215 ± 1	≥ 500
	4	≤ 500	≥ 500	380 ± 27	≥ 500	200 ± 1	≥ 500
GM113	1	≥ 300	≥ 300	≥ 300	≥ 300	33 ± 1	≥ 300
	4	≥ 300	≥ 300	≥ 300	≥ 300	21 ± 1	≥ 300
GM508	1	84 ± 1	≥ 300	≥ 300	≥ 300	69 ± 1	≥ 300
	4	74 ± 1	≥ 300	≥ 300	≥ 300	50 ± 1	≥ 300

Tetrahydroisoquinoline moiety did not trigger a release of LDH

Release of LDH was analyzed in cells exposed for 4 hours to a range of aldoxime concentrations and the results are presented in Fig. 2. There was no LDH release recorded after cell-exposure to these aldoximes, compared to untreated cells, except highest concentration of GM415 on HEK293. Also, results obtained here were similar for every cell line tested.

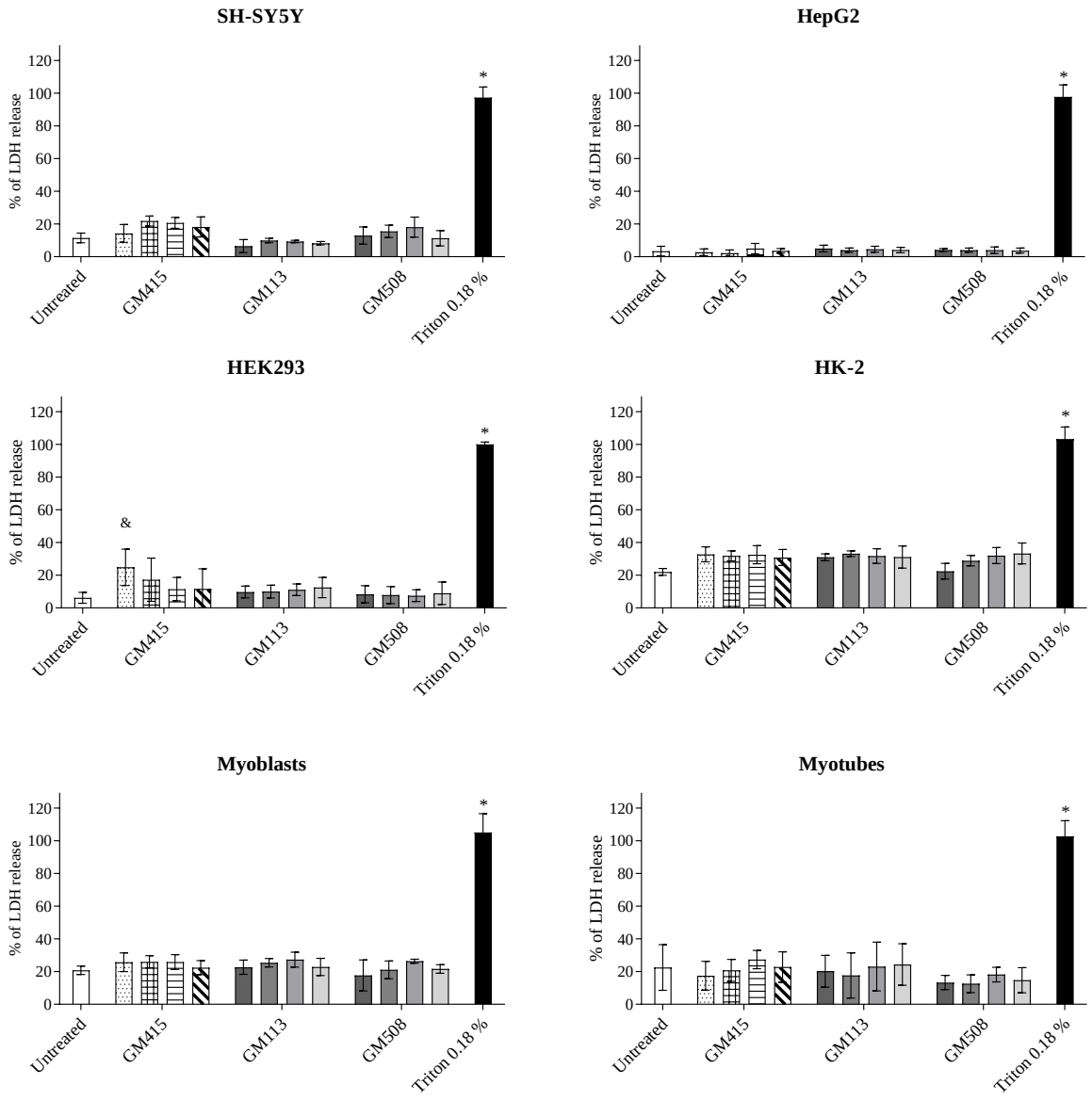

Fig. 2 Levels of LDH release after 4-hour exposure to selected compounds: 62.5 – 500 µM (GM415), 37.5 – 300 µM (GM113 and GM508) for SH-SY5Y, HepG2, HEK293, HK-2, myoblasts, and myotubes. Statistical significance: Ordinary one-way ANOVA Bonferroni's multiple comparisons test to the untreated cells (&$p < 0.05$, *$p < 0.0001$). Triton X-100 (0.18 %) was used as a positive control to generate maximal LDH release in the culture medium. Legend: white – untreated cells, red – positive control, dark orange – 300 µM, orange – 150 µM, light orange – 75 µM, beige – 37.5 µM, or dark turquoise – 500 µM, turquoise – 250 µM, light turquoise – 125 µM, light blue – 62.5 µM

Based on the obtained results presented in Table 1, toxicity on SH-SY5Y, HepG2 and HEK293 cells was in the same concentration range (same order of magnitude) and follow the same pattern implying similar mechanism of action. From these three cell types, neuronal cells SH-SY5Y have been chosen as the model for further evaluation since they carry the primary target of tested compounds (AChE enzyme) and have lower expression of phase I and phase II metabolic enzymes than the liver or kidney cells, which can influence final results (Lock and Reed 1998; Hewitt and Hewitt 2004).

Tetrahydroisoquinoline aldoximes induced reactive oxygen species and disrupted mitochondrial membrane potential $\Delta\Psi_m$

Induction of reactive oxygen species (ROS) was measured on SH-SY5Y cells after 4-hour exposure to aldoximes at LOAEL (Lowest-observed-adverse-effect level) concentrations, and obtained results are presented in Fig. 3A. As results indicate, aldoximes GM415 and GM113 significantly increased levels of ROS (Fig. 3A), while aldoxime GM508 (additional 4-(dimethylamino)phenyl moiety in the structure) did not.
Disruption of mitochondrial membrane potential ($\Delta\Psi_m$) may cause undesired changes in the cell homeostasis, including an increase in ROS production; therefore, we determined change in $\Delta\Psi_m$ in living SH-SY5Y cells exposed to selected 3-hydroxy-2-pyridine aldoximes for 4 hours (Fig. 3B). As results show, statistically significant increase of $\Delta\Psi_m$ was observed for all tested aldoximes compared to the untreated cells.

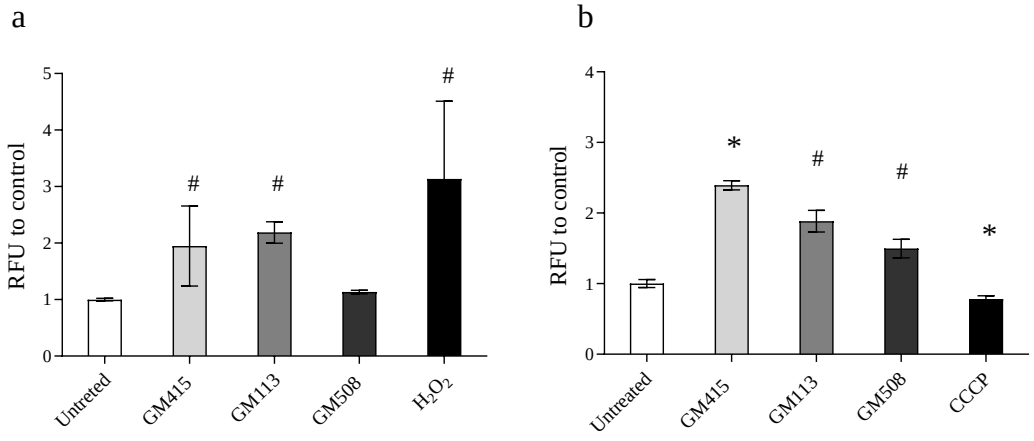

Fig. 3 (a) The measured DCF-fluorescence signal indicating ROS level after 4-hour exposure to LOAEL concentration of selected aldoximes; GM415 (350 µM, orange), GM113 (300 µM, light orange) and GM508 (50 µM, dark turquoise) in SH-SY5Y cells. Statistical significance: Ordinary one-way ANOVA - Holm-Sidak (#$p < 0.01$). H_2O_2 (100 µM, red) was used as a positive control. **(b)** Mitochondrial membrane potential determined by TMRE after 4-hour exposure to the LOAEL concentration of the selected aldoximes: GM415 (350 µM, orange), GM113 (300 µM, light orange) and GM508 (50 µM, dark turquoise) in SH-SY5Y cells. Statistical significance: Ordinary one-way ANOVA – Dunnett's test. (#$p < 0.01$; *$p < 0.0001$). CCCP (50 µM, red) was used as a positive control inducing a decrease of $\Delta\Psi_m$ compared to the untreated cells. Results are presented as relative fluorescence units (RFU) to untreated cells.

Tetrahydroisoquinoline-based 3-hydroxy-2-pyridine aldoximes cause synergistic toxic effects

We exposed SH-SY5Y cells for 4 hours to a pair of 3-hydroxy-2-pyridine aldoximes present in their respective LOAEL concentration, to investigate a potential synergistic effect. Synergistic toxicity was detected only in the combination of GM415 and GM508, at LOAEL concentrations, where this combination killed almost 80 % of the cells (Fig. 4).

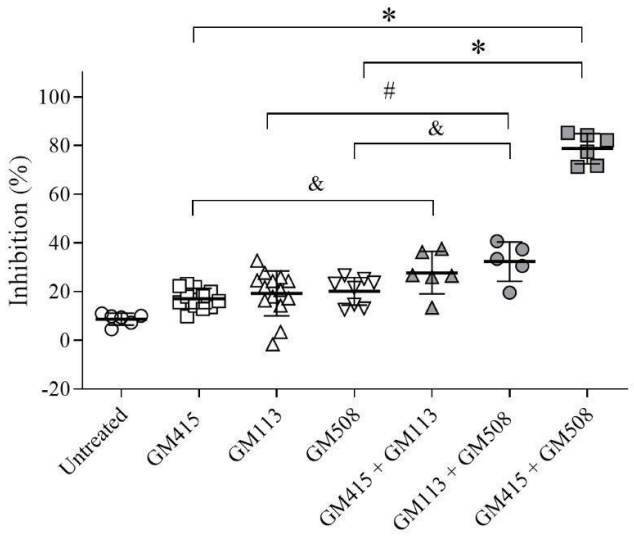

Fig. 4 Synergistic toxicity evaluated by MTS assay and presented as percentage of inhibition of cell viability after 4-hour exposure to LOAEL concentration of selected aldoximes: GM415 (350 µM), GM113 (300 µM), GM508 (50 µM) and their combinations in SH-SY5Y cells. Statistical significance: Ordinary one-way ANOVA – Dunnett's test (&p < 0.05; #p < 0.01; *p < 0.0001)

Tetrahydroisoquinoline based 3-hydroxy-2-pyridine aldoximes activate apoptosis while aldoxime with additional phenyl moiety caused DNA damage

The activation and activity of specific apoptosis markers were evaluated after 4-hour exposure of SH-SY5Y cells to aldoximes at LOAEL concentration. According to the results, GM113 and GM508 induced early apoptotic events (Fig. 5a). However, when the total number of apoptotic cells was compared, all tested aldoximes led to apoptosis (Fig. 5b). One of the triggering events that lead to apoptosis, can be DNA damage. Therefore, the total double-stranded DNA damage in cells was estimated after 4-hour exposure to aldoximes by measuring activated kinase ATM and phosphorylated histone H2A.X. According to the results, only GM113 caused a statistically significant increase in DNA damage. An increase in damage was also observed after GM508 treatment but was not statistically significant (Fig. 5c).

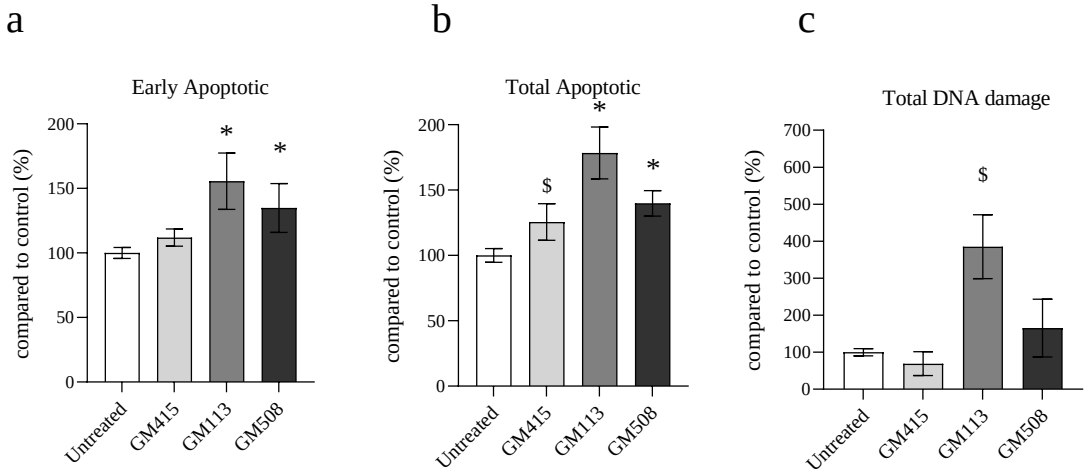

Fig. 5 (a) The percentage of early and total apoptotic cells compared to the untreated cells after 4-hour exposure to LOAEL concentration of selected aldoximes; GM415 (350 µM, orange), GM113 (300 µM, light orange) and GM508 (50 µM, dark turquoise) in SH-SY5Y cells. Paraformaldehyde (0.08%) was used as a positive control with values 290 % and 298 % for early and total apoptotic cells, respectively (due to a clearer presentation, these values for the positive control are not shown in the graph). (**b)** Total DNA damage in SH-SY5Y cells after 4-hour exposure to the LOAEL concentration of the selected aldoximes: GM415 (350 µM, orange), GM113 (300 µM, light orange) and GM508 (50 µM, dark turquoise). Etoposide (10 µM) was used as a positive control with mean value of 878.45% for DNA damage (due to a clearer presentation, these values for the positive control are not shown in the graph). Statistical significance: Ordinary one-way ANOVA – Dunnett's test. ($p < 0.001; *p < 0.0001). Results are presented as percent of apoptotic cells or total DNA damage in cells compared to the untreated cells.

To confirm that these aldoximes activate regulated cell death, the activity of three specific caspases was measured, and the results are presented in Fig. 6. All tested aldoximes activated the initiator caspase 9, indicating mitochondria-mediated activation of the apoptosis, while GM508 additionally activated caspase 8, indicating receptor-mediated cell death. Both initiator caspases participate in the induction of cascade responsible for activation of regulated cell death. Furthermore, the three tetrahydroisoquinoline-based 3-hydroxy-2-pyridine aldoximes activated the most important executor caspase 3.

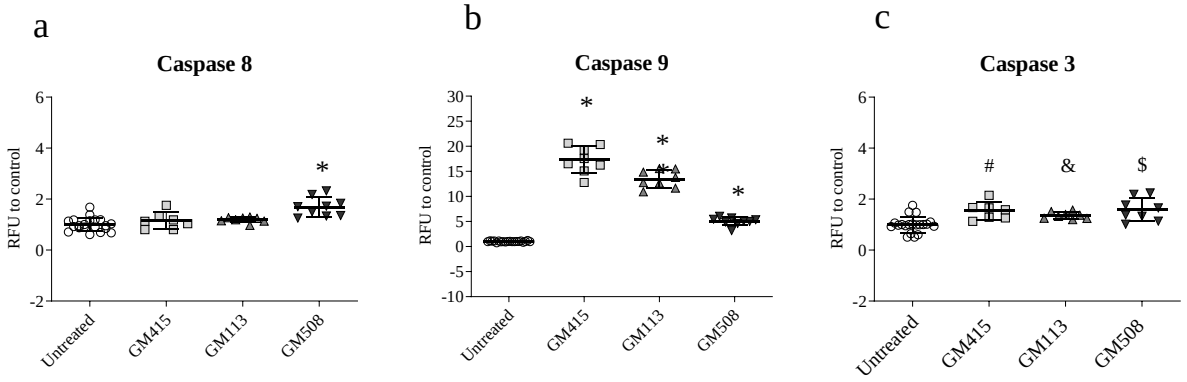

Fig. 6 Specific caspase activity: (**a**) caspase 8, (**b**) caspase 9 and (**c**) caspase 3 in SH-SY5Y cells after 4-hour exposure to the LOAEL concentration of the selected aldoximes; GM415 (350 µM), GM113 (300 µM), GM508 (50 µM). Statistical significance: Ordinary one-way ANOVA – Dunnett's test. (&p < 0.05; #p < 0.01; $p < 0.001; *p < 0.0001). Results are presented as relative fluorescence units (RFU) to untreated cells. Staurosporine (3 µM) was used as a positive control and initiated activation of caspases 3, 8 and 9 (Zandona et al. 2021)

Tetrahydroisoquinoline-based 3-hydroxy-2-pyridine aldoximes translocate across the blood-brain barrier model

We analyzed the *in silico* physicochemical properties of the selected aldoximes important for passing through biological membranes. Data for physicochemical properties for GM415 and GM508 were reported previously (Zorbaz et al. 2018) and data for GM113 is given here (Table S1). According to the recommended values from the literature (Pajouhesh and Lenz 2005), these three 3-hydroxy-2-pyridine aldoximes are not considered as candidates for passive penetration through membranes, due to the high number of rotatable bonds (RB), the octanol-water partition coefficient (clogP), topological polar surface area (TPSA) and molecular weight (M) values (Table S1).
In order to verify *in silico* predictions, *in vitro* experiments were performed to determine whether GM415, GM113, and GM508 pass through endothelial cell barrier model (HBEC-5i) and whether they are substrates of P-glycoprotein (P-gp) pumps on MDCKII-MDR1 model with overexpressed P-gp efflux pumps. Obtained results are summarized in Table 4 and Fig. 7. As results indicate, all tested aldoximes are considered to be substrates of the P-gp efflux transporter (Table 4).

Table 4 Permeability from the apical to basolateral side P_{app} (AB) and P_{app} (BA) from the basolateral to apical side, and efflux ratio (ER) of tested aldoximes with (+) or without (-) P-gp inhibitor elacridar in the MDCKII-MDR1 cell line

Aldoxime	Elacridar	P_{app} (A2B)	P_{app} (B2A)	ER[a]
GM415	-	4.6	40.9	9.5
	+	21.3	25.3	1.2
GM113	-	0.4	10.5	21.2
	+	4.8	7.0	1.7
GM508	-	0.8	16.1	23.2
	+	3.9	3.6	0.9

[a] A compound is considered to be a P-gp substrate when the efflux ratio (ER) in the absence of inhibitor elacridar is >2, while is significantly reduced (≥ 50%) in its presence.

According to the determined strong cytotoxic effect of tested aldoximes on HBEC-5i cells (IC_{50} in 24 hours were 240 μM, 14 μM and 10 μM, and in 4 hours ≥ 500 μM, 178 μM and 105 μM for GM415, GM113 and GM508, respectively), the concentrations of aldoximes for BBB translocation assay were selected separately from other performed experiments on cells to avoid paracellular leakage of BBB model and overestimation of aldoximes passing through the cell barrier especially in 4 h exposure time. Results indicate that the translocation of tested aldoximes was up to 40 % in 4 hours, and up to 55 % in 24 hours (Fig. 7). Furthermore, except for the percentage of retention (i.e. residual aldoxime in the cells or on the transwell filter) was up to 56 % and 42 % in 4 and 24 hours (Fig. 7), respectively.

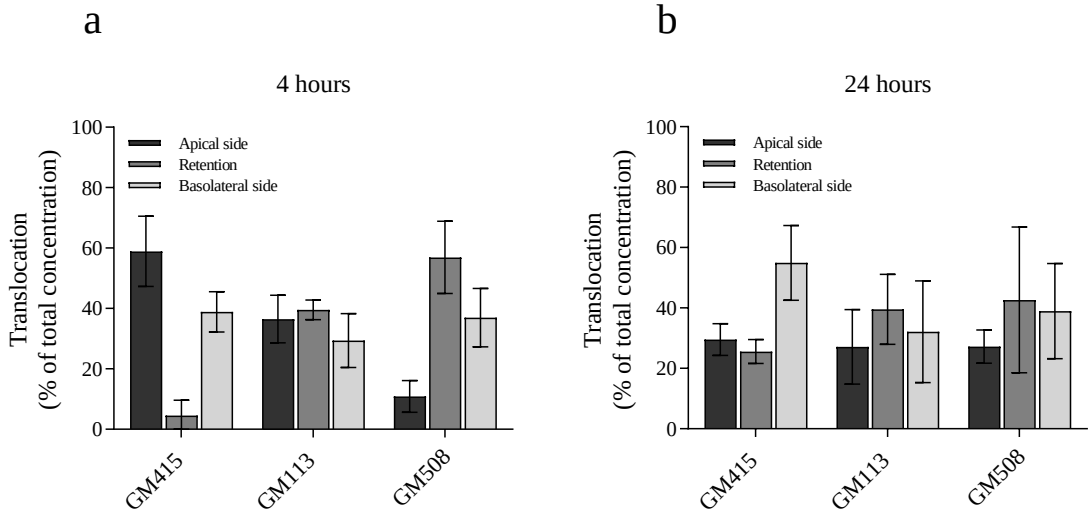

Fig. 7 Translocation of aldoximes across HBEC-5i *in vitro* BBB model after (**a**) 4 hours and (**b**) 24 hours: GM415 (200 μM), GM113 (50 μM), GM508 (15 μM) and 24 hours: GM415 (50 μM), GM113 (3 μM), GM508 (5 μM). Results are presented as total concentration of aldoximes passed through BBB membrane model, apical side (orange), retention (light orange) and basolateral side (dark turquoise). The membrane integrity was high (above 85 %) and did not differ from untreated cells, meaning that the experiments were successful and the values represent translocation through the intact BBB (data not shown)

Tetrahydroisoquinoline-based 3-hydroxy-2-pyridine aldoximes increase phosphorylation of ERK1/2, p38-MAPK, and ACC, and decrease phosphorylation of NFκB and STAT3

Specific mechanism of cytotoxicity was investigated in more detail by analyzing signaling in SH-SY5Y cells. Several targets of the most important signaling pathways involved in cell growth, proliferation, metabolism, and survival were followed. Results are shown in Fig. 8. The phosphorylation of extracellular signal-regulated kinase (ERK1/2), which regulates several stimulated cellular processes, was significantly increased by tested compounds depending on the structure and time point of activation. GM415 and GM508 suppressed phosphorylation of nuclear factor-κB (NF-κB), transcription factor involved in inflammatory responses. Furthermore, all three aldoximes increased phosphorylation of p38 mitogen-activated protein kinase (p38-MAPK), sensitive to stress stimuli involved in apoptosis, after 30 minutes or more. Interestingly, phosphorylation of transcription factor STAT3, which plays a key role in many cell

processes, especially in cell growth and apoptosis, was significantly decreased after being exposed to tested aldoximes, while only 5 minutes after being exposed to GM113 and GM508 it was increased. Additionally, the level of phosphorylation of AMP-activated protein kinase (AMPK), a cellular energy sensor, was neither significantly increased nor decreased, while the phosphorylation of its downstream substrate acetyl-CoA carboxylase (ACC) was significantly increased during the whole exposure period (Fig. 8).

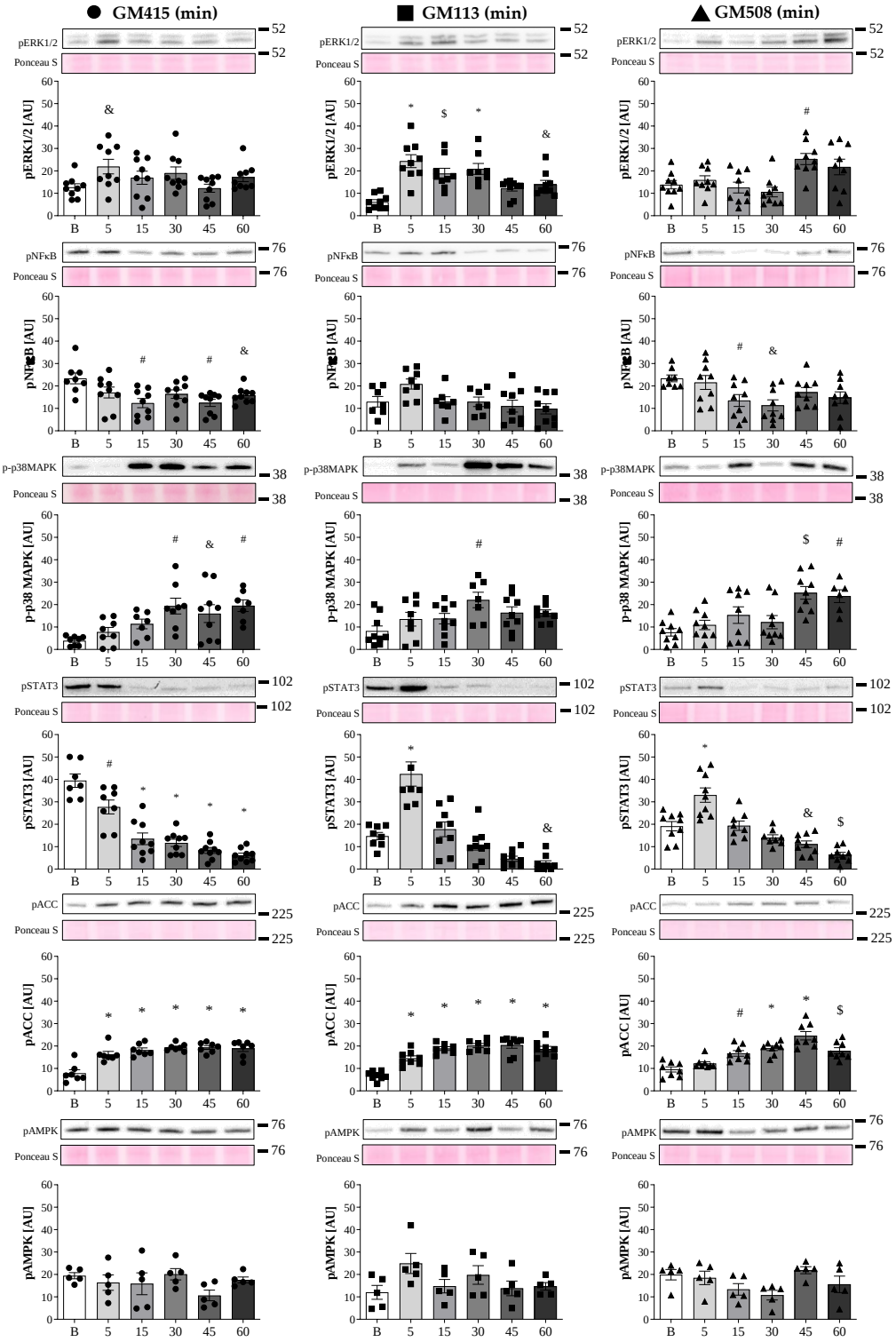

Fig. 8 Effects of GM415 (350 μM), GM113 (300 μM) and GM508 (50 μM) on phosphorylation of ERK1/2, NFκB, p38 MAPK, STAT3, ACC and AMPK in 5, 15, 30, 45 and 60 minutes exposure of SH-SY5Y cells. Results are means ± SD (n = 5–9). Statistical significance: Unpaired one-way ANOVA – Dunnett's test (&p < 0.05; #p < 0.01; $p < 0.001; *p < 0.0001 vs. basal (B)

In silico analysis and pharmacophore model predicted potential targets for tetrahydroisoquinoline-based 3-hydroxy-2-pyridine aldoximes

To predict potential cell targets interacting with three selected 3-hydroxy-2-pyridine aldoximes, we used a SwissTargetPrediction software (Daina et al. 2019). For all tested aldoximes the top 15 % target class frequency were found to be kinases, and the second target class pointed as probable were G-protein coupled receptors (Fig. S1). Also, in the analysis, aldoximes of this structure were not classified as PAINS (Pain-Assay-Interference-Compounds, Fig. S1), (Davis and Erlanson 2013; Baell and Walters 2014)). Furthermore, we generated a corresponding pharmacophore model and ran a drug similarity search through the public database to check if any alike registrated compound exists. According to the protocol, we marked GM415, GM113, and GM508 as active based on the IC_{50} values (cf. Table 2). Fig. 9a illustrates 3-hydroxy-2-pyridine aldoxime GM508 mapped onto the final pharmacophore model. Next, we screened databases to identify ligands in a database that best map to the generated pharmacophore. In the case of the pharmacophore model for GM508, (1R,3S,5R,7S)-N-[8-({[5-(dimethylamino)naphtalen-1-il]sulphonil}amino)octil]-3hydroxytriciklo[3.3.1.1~3,7~] decan -1-carboxamid was singled out as the most interesting result (Fig. 9b) – inhibitor of cytochrome P450 –CYP101A from *Pseudomonas putida*, bacterial form of CYP, involved in diverse metabolic processes. Interestingly, additional *in silico* analysis using the online platform SwissADME (Daina et al. 2017) predicted also interactions of tested compounds with human cytochrome enzymes (Table S2). Here, out of five major human CYP isoforms, inhibition of CYP2D6 and CYP3A4 could be achieved by all tested aldoximes, while only GM508 could inhibit CYP2C19 (Table S2).

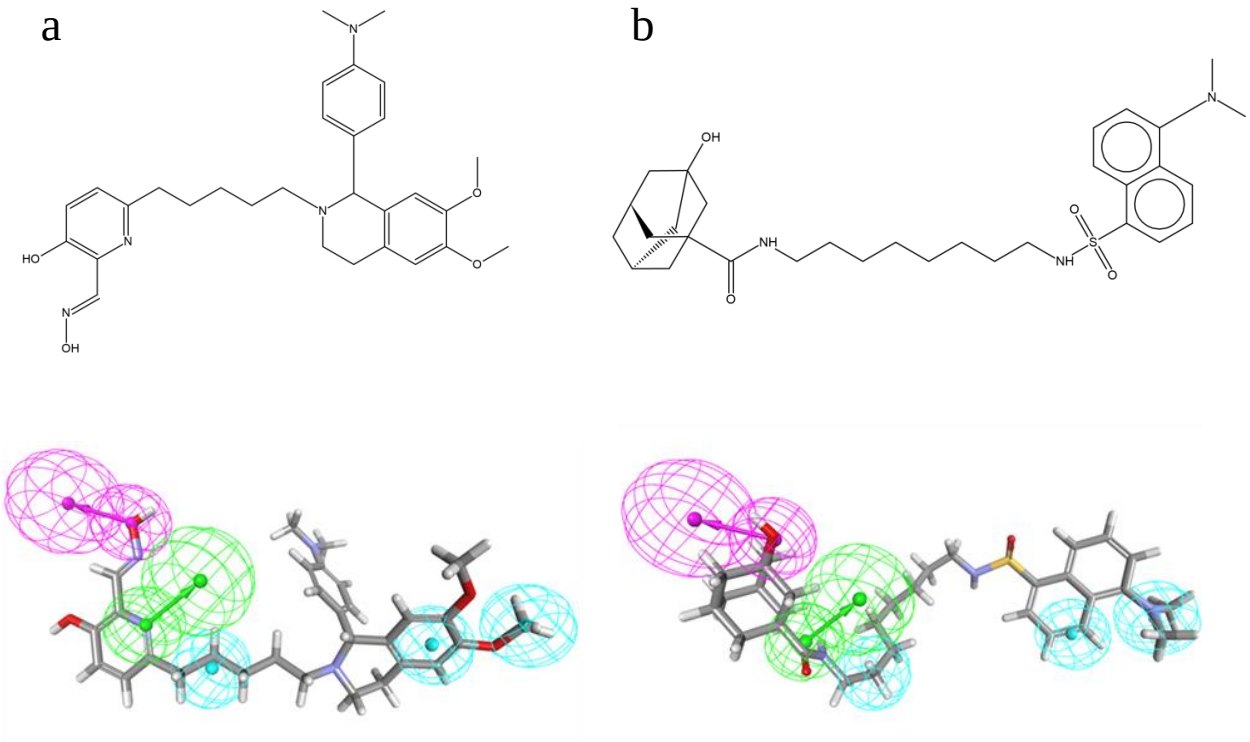

Fig. 9 (**a**) GM508 mapped onto the pharmacophore model for 3-hydroxy-2-pyridine aldoximes. (**b**)(1R,3S,5R,7S)-N-[8-({[5-(dimethylamino)naphtalen-1-il]sulphonil}amino)octil]-3-hydroxytriciclo [3.3.1.1~3,7~] decan-1-carboxamide mapped onto the pharmacophore model for 3-hydroxy-2-pyridine aldoxime. Green spheres represent hydrogen bond acceptor features; magenta spheres represent hydrogen bond donor features; blue spheres represent hydrophobic features

Discussion

In this study, we investigated four uncharged 3-hydroxy-2-pyridine aldoximes, designed as OP-inhibited acetylcholinesterase reactivators, as candidates for drug development. According to the results, we were pleased to observe that aldoxime with a piperidine moiety, JR585, showed no toxicity on any of the cells tested within 24-hour exposure, confirming previous results (Zorbaz et al. 2018, 2020). As it had already been reported efficient in reactivation of AChE, this result strengthens its consideration as a good scaffold for organophosphorus-poisoning antidotes development (Zorbaz et al. 2018, 2020). In contrast, three tetrahydroisoquinoline-based 3-hydroxy-2-pyridine aldoximes (GM415, GM113, GM508) caused cytotoxicity on every tested cell type in the studied concentration range. The addition of the phenyl (GM113) or 4-(dimethylamino)phenyl moieties (GM508), on such aldoximes, increased the cytotoxicity from 3 up to 24-fold (see Table 2). The detailed cytotoxicity analysis, after 1- and 4-hour exposure period, revealed time-dependent effects triggered by aldoximes, leading to cell death within 24 hours (cf. Table 2 and 3). Furthermore, aldoximes GM415 and GM508 caused a synergistic cytotoxic effect resulting in a higher toxicity when applied together in comparison with individually observed cytotoxicity (see Fig. 4). Such time-dependent and synergistic effects are similar to ones obtained for several bispyridinium oximes and imidazolium-based oximes, respectively, which indicates that the toxicity of such type of compounds could be associated to the same mechanisms (Zandona et al. 2021). By checking the influence of 3-hydroxy-2-pyridine aldoximes on the membrane integrity, it has been shown that they do not cause dose-dependent LDH leakage that would indicate their mechanism of action solely by affecting membrane integrity per se (see Fig. 2). Somewhat preserved membrane integrity without direct necrosis accompanied by time-dependent cytotoxicity could indicate regulated cell death as aldoximes' mechanism of action on cells (Suzuki et al. 2004). This was detected here, in the studied time frame, only for aldoximes with tetrahydroisoquinoline moieties (GM415, GM113, GM508). They activated regulated cell death - apoptosis by translocation of phosphatidylserine on the external membrane of early apoptotic cells and by permeabilization/disruption of membranes in the late stages of the apoptotic process (cf. Fig. 5) (Chaurio et al. 2009). Furthermore, these aldoximes activated initiator caspase 9, which is essential for apoptosis signaling through the intrinsic mitochondria-dependent pathway (see Fig. 6b) (Li et al. 2017). Observed induction of ROS indicating an increase in oxidative stress (see Fig. 3a) and alteration in the mitochondrial membrane potential, (Fig. 3b), could be the reasons for activating cascade that led to the activation of caspase 9 (Brentnall et al. 2013). Namely, mitochondrial damage by increased ROS level leads to release of cytochrome c into the cytoplasm and activates caspase 9 (Zou et al. 2013). On the other hand, it seems that presence of 4-(dimethylamino)phenyl group (GM508) was responsible for the additional activation of the initiator caspase 8 (Wu et al. 2016), via the extrinsic pathway. Interestingly, induction of ROS and activation of caspase 8 is usually triggered by a mechanism involving receptors associated with tumor necrosis factors (TNFs) (Tummers and Green 2017). This could mean that GM508 interacts with TNFs on the cell surface as well. Anyhow, both caspases, 8 and 9, activate executor caspase 3 as has been observed in our results as well, which triggers apoptosis through cleavage of many downstream proteins (Hengartner 2000). In addition, GM113 caused DNA damage (see Fig. 5c) which can be another trigger of regulated cell death (Roos and Kaina 2006; Kryston et al. 2011).

These aldoximes are synthesized as uncharged molecules with the aim to enhance their passive transport through the BBB and the biological membranes (Bodor et al. 1975; Koichi Sakurada , Kazuo Matsubara, Keiko Shimizu, Hiroshi Shiono, Yasuo Seto, Koichiro Tsuge, Mineo Yoshino, Ikuko Sakai, Harutaka Mukoyama 2003; Lorke et al. 2008; Zorbaz et al. 2018; Rosenberg et al. 2018), so they could enter the cells and trigger specific processes from within. In other words, the presumed mechanism of action of aldoximes also depends on their ability to enter/exit the cell (Mandel 1986; Forrest et al. 2011). Therefore, we tested their permeation *in silico* and *in vitro* to estimate such prediction. Based on *in silico* data, tetrahydroisoquinoline-based 3-hydroxy-2-pyridine aldoximes GM415, GM113 and GM508 are not ideal candidates for passive diffusion through the membranes Table S1. Even though *in silico* analysis did not mark selected aldoximes as favorable for passive permeation, *in vitro* parallel artificial membrane permeability assay (PAMPA) showed differently (Zorbaz et al. 2018). Since the PAMPA membrane is composed only of chosen and selected lipids (Ribeiro et al. 2010), we wanted to investigate aldoxime's active translocation further in a more realistic system; on a model composed of human brain endothelial cells cultured in a monolayer (Cavaco et al. 2020b). Also, the probability of efflux of aldoximes by P-glycoprotein (P-gp) pumps was checked in MDCKII-MDR1 cells with overexpressed multidrug resistance protein 1 (MDR1 i.e. P-gp) gene (Polli et al. 2001; Desai et al. 2012). Specifically, P-gp pumps are responsible for the elimination of drugs from cells in the liver, kidney and at the BBB (Fromm 2004). This is even more important since it is expected that such oximes are removed from the organism by renal excretion (Handl et al. 2021) and in here presented study they showed significant toxicity toward kidney cells. As results show, tested aldoximes were able to translocate in a high percentage through HBEC-5i model (see Fig. 7), regardless of being P-gp substrates. This indicates that aldoximes could act in the cell over time, since they will not be completely removed by the efflux pumps.

Further on, with an aim to clarify the possible mechanism behind cytotoxicity, we checked phosphorylation of several cell targets. We observed the increased phosphorylation of kinases ERK 1/2 and p38 MAPK after aldoxime treatment which indicates the influence of aldoximes on the cell homeostasis (Roux and Blenis 2004; Alvarado-Kristensson and Andersson 2005). Increased phosphorylation of MAPK could be a result of aldoximes binding to acetylcholine

receptors AChR (nicotinic and especially muscarinic G-coupled receptors) (Jiménez and Montiel 2005; Arora et al. 2015). Binding of oximes to these receptors has been shown previously by other researchers studying new drugs for neurodegenerative disorders (e.g. Alzheimer's disease) (Soukup et al. 2013; Hepnarova et al. 2019). However, it could be just a result of disturbed mitochondrial membrane potential, elevated ROS levels or DNA damage, which was caused by aldoximes with a tetrahydroisoquinoline moiety. Interestingly, activated ERK1/2 and p38 MAPK can also activate caspase 9 and caspase 3 and consequently induce apoptosis (Alvarado-Kristensson and Andersson 2005), as perceived in this study. On the other hand, due to the suppressed phosphorylation of the NFκB protein complex, the expression of anti-apoptotic factors, such as Bcl-2 (Abbaspour Babaei et al. 2017), probably does not occur. As mentioned, these aldoximes can potentially act on tumor necrosis factor receptors (TNFRs), and its inhibition can lead to a decrease in phosphorylation of downstream substrates such as NFκB and consequently cell death (Van Quickelberghe et al. 2018). Furthermore, phosphorylation of transcription factor STAT3 was increased only in the first 5 minutes of treatment, concomitant with increase of protein transcription necessary for cell survival. However, after 5 minutes there was a significant decrease in STAT3 phosphorylation leading to apoptosis (Ma et al. 2020). In addition, we observed elevated phosphorylation of ACC, an important enzyme in the de novo synthesis of fatty acids in the cytoplasm and β-oxidation of fatty acids in mitochondria (Saggerson 2008), potentially due to mitochondrial membrane disruption potential and activation of mitochondrial apoptotic pathway (see Fig. 3b and 6b). Interestingly, no phosphorylation of AMPK has been noticed, which otherwise phosphorylates ACC, thus leading to its inhibition and an increase in fatty acid oxidation. Fediuc et al suggested that regulation of ACC does not depend only on AMPK phosphorylation (Fediuc et al. 2006), which could be the case in this study and certainly is interesting to further investigate.

Additionally, we analysed *in silico* probability of aldoximes interactions with biological targets and the results pointed to kinases and/or G-coupled protein receptors (GPCRs). Interestingly, our previous research on pyridinium oximes showed that compounds like these indeed interact with cholinergic receptors, one of which are the muscarinic GPCRs, which might be also the case here. Furthermore, we screened the known databases according to the pharmacophore model to find similar compounds with defined targets which could also be potential targets of our aldoximes' action (see Fig. 9). Specifically, the pharmacophore model provides important information regarding three-dimensional arrangement of steric and electronic features necessary for establishing key interactions with biological target which elicit observed biological response or measured activity (Gaurav and Gautam 2014; Johnson and Karanicolas 2016). Based on the pharmacophore model (Zandona et al. 2021) high similarity was found only with the inhibitor of cytochrome P450 – CYP101A from *Pseudomonas putida*, the bacterial form of CYP (OuYang et al. 2008). Due to the uniformity of structures and gene conservation within the cytochrome P450 family (Hasemann et al. 1995), there is a possibility of inhibition of human cytochromes with tetrahydroisoquinoline-based 3-hydroxy-2-pyridine aldoximes as well. So, we checked this hypothesis by *in silico* prediction analysis. We focused on the probability of aldoximes inhibiting the most common human CYPs, responsible for xenobiotic metabolism in the body (Sychev et al. 2018; Esteves et al. 2021). For our aldoximes, interactions were predicted with cytochrome CYP2D6, CYP3A4 and/or CYP2C19. Consequently, if true, this may directly reduce the ability of CYPs to metabolize compounds and influence in a way their toxicity (Esteves et al. 2021). Furthermore, P-gp pumps are known to have a similar spectrum of substrates as CYP3A4 (König et al. 2013), which would further suggest that tetrahydroisoquinoline-based 3-hydroxy-2-pyridine aldoximes could interact with CYP enzymes. Additionally, it is shown that some of these aldoximes interact with CYPs and were resistant to oxidative metabolism while GM508 showed rapid degradation or biotransformation (Zorbaz et al. 2020). However, such and all other predicted interactions should be elucidated in the future by additional specific *in vitro* experiments.

Conclusions

Our results indicate that differences in the structures of 3-hydroxy-2-pyridine aldoximes affect their effects on the cell level. Indeed, only three compounds with a tetrahydroisoquinoline moiety showed a significant toxicity, in a cell-type independent manner. Furthermore, they caused the activation of a reaction cascade that consequently led to the activation of regulated cell death, by caspase-dependent apoptosis. At the same time, the suppression of anti-apoptotic genes contributed to this mechanism. Overall, observed biological activity of aldoximes with tetrahydroisoquinoline moiety could be indicative for future design of compounds either in a negative context in OP antidotes design, or in a positive one for the design of compounds for the treatment of other conditions and diseases. In other words, the researchers including similar compounds in their studies could either benefit from their non-antidotal biological activity or should be aware that they might influence cells and that it would be desirable to analyze such effects before any advanced studies, especially those *in vivo*. In that manner, the structure of non-toxic aldoxime JR585 could be further considered for OP-antidote development, while, observed influence on cells could make 3-hydroxy-2-pyridine

aldoximes the starting compounds for investigating interactions with specific targets for instance, in the treatment of cancer, where aldoximes could be used to induce apoptosis in tumor cells.

Author Contributions: Conceptualization, A.Z. and M.K.; methodology, A.Z., J.M., K.M., Ma.C. and P.M.; software, N.M.; validation, J.P., Mi.C., S.P., V.N. and M.K.; formal analysis, A.Z., K.M.; investigation, A.Z., J.M., K.M., Ma.C. and P.M. ; resources, Mi.C., P.-Y.R., S.P., V.N. and M.K.; writing—original draft preparation, A.Z., J.M. and M.K.; writing—review and editing, A.Z., J.M., K.M., N.M., P. D.-G., Ma.C., J.P., Mi.C., L.J., P.-Y.R, S.P., V.N. and M.K.; visualization, A.Z., K.M., N.M.; supervision, Mi.C., P.-Y.R., S.P., V.N. and M.K.; project administration, M.K; funding acquisition, M.K. All authors have read and agreed to the published version of the manuscript.

References

Aas V, Bakke SS, Feng YZ, et al (2013) Are cultured human myotubes far from home? Cell Tissue Res 354:671–682. https://doi.org/10.1007/s00441-013-1655-1

Abbaspour Babaei M, Zaman Huri H, Kamalidehghan B, et al (2017) Apoptotic induction and inhibition of NF-κB signaling pathway in human prostatic cancer PC3 cells by natural compound 2,2'-oxybis (4-allyl-1-methoxybenzene), biseugenol B, from Litsea costalis: an in vitro study. Onco Targets Ther Volume 10:277–294. https://doi.org/10.2147/OTT.S102894

Abdelmoez AM, Sardón Puig L, Smith JAB, et al (2020) Comparative profiling of skeletal muscle models reveals heterogeneity of transcriptome and metabolism. Am J Physiol Physiol 318:C615–C626. https://doi.org/10.1152/ajpcell.00540.2019

Alvarado-Kristensson M, Andersson T (2005) Protein phosphatase 2A regulates apoptosis in neutrophils by dephosphorylating both p38 MAPK and its substrate caspase 3. J Biol Chem 280:6238–6244. https://doi.org/10.1074/jbc.M409718200

Arora K, Cheng J, Nichols RA (2015) Nicotinic acetylcholine receptors sensitize a MAPK-linked toxicity pathway on prolonged exposure to β-amyloid. J Biol Chem 290:21409–21420. https://doi.org/10.1074/jbc.M114.634162

Baell J, Walters MA (2014) Chemistry: Chemical con artists foil drug discovery. Nature 513:481–483. https://doi.org/10.1038/513481a

Bodor N, Shek E, Higuchi T (1975) Delivery of a quaternary pyridinium salt across the blood-brain barrier by its dihydropyridine derivative. Science (80-) 190:155–156. https://doi.org/10.1126/science.1166305

Bouma ME, Rogier E, Verthier N, et al (1989) Further cellular investigation of the human hepatoblastoma-derived cell line HepG2: Morphology and immunocytochemical studies of hepatic-secreted proteins. Vitr Cell Dev Biol 25:267–275. https://doi.org/10.1007/BF02628465

Brentnall M, Rodriguez-Menocal L, De Guevara RL, et al (2013) Caspase-9, caspase-3 and caspase-7 have distinct roles during intrinsic apoptosis. BMC Cell Biol 14:32. https://doi.org/10.1186/1471-2121-14-32

Calas A-G, Dias J, Rousseau C, et al (2017) An easy method for the determination of active concentrations of cholinesterase reactivators in blood samples: Application to the efficacy assessment of non quaternary reactivators compared to HI-6 and pralidoxime in VX-poisoned mice. Chem Biol Interact 267:11–16. https://doi.org/10.1016/j.cbi.2016.03.009

Cavaco M, Frutos S, Oliete P, et al (2021) Conjugation of a blood brain barrier peptide shuttle to an Fc domain for brain delivery of therapeutic biomolecules. ACS Med Chem Lett 12:1663–1668. https://doi.org/10.1021/acsmedchemlett.1c00225

Cavaco M, Pérez-Peinado C, Valle J, et al (2020a) To what extent do fluorophores bias the biological activity of peptides? A practical approach using membrane-active peptides as models. Front Bioeng Biotechnol 8:. https://doi.org/10.3389/fbioe.2020.552035

Cavaco M, Valle J, da Silva R, et al (2020b) D PepH3, an improved peptide shuttle for receptor-independent transport across the blood-brain barrier. Curr Pharm Des 26:1495–1506. https://doi.org/10.2174/1381612826666200213094556

Chaurio R, Janko C, Muñoz L, et al (2009) Phospholipids: Key players in apoptosis and immune regulation. Molecules 14:4892–4914. https://doi.org/10.3390/molecules14124892

Daina A, Michielin O, Zoete V (2017) SwissADME: A free web tool to evaluate pharmacokinetics, drug-likeness and medicinal chemistry friendliness of small molecules. Sci Rep 7:1–13. https://doi.org/10.1038/srep42717

Daina A, Michielin O, Zoete V (2019) SwissTargetPrediction: updated data and new features for efficient prediction of protein targets of small molecules. Nucleic Acids Res 47:W357–W364. https://doi.org/10.1093/nar/gkz382

Davis BJ, Erlanson DA (2013) Learning from our mistakes: The 'unknown knowns' in fragment screening. Bioorg

Med Chem Lett 23:2844–2852. https://doi.org/10.1016/j.bmcl.2013.03.028
Decker T, Lohmann-Matthes M-L (1988) A quick and simple method for the quantitation of lactate dehydrogenase release in measurements of cellular cytotoxicity and tumor necrosis factor (TNF) activity. J Immunol Methods 115:61–69. https://doi.org/10.1016/0022-1759(88)90310-9
Desai P V, Raub TJ, Blanco M (2012) Bioorganic & Medicinal Chemistry Letters How hydrogen bonds impact P-glycoprotein transport and permeability. Bioorg Med Chem Lett 22:6540–6548. https://doi.org/10.1016/j.bmcl.2012.08.059
Dolinar K, Jan V, Pavlin M, et al (2018) Nucleosides block AICAR-stimulated activation of AMPK in skeletal muscle and cancer cells. Am J Physiol Cell Physiol 315:C803–C817
Dulbecco R, Vogt M (1954) Plaque formation and isolation of pure lines with poliomyelitis viruses. J Exp Med 99:167–182. https://doi.org/10.1084/jem.99.2.167
ECACC (2017) Fundamental techniques in cell culture laboratory handbook 4th edition. Merck KGaA
Esteves F, Rueff J, Kranendonk M (2021) The central role of cytochrome P450 in xenobiotic metabolism—A brief review on a fascinating enzyme family. J Xenobiotics 11:94–114. https://doi.org/10.3390/jox11030007
Fediuc S, Gaidhu MP, Ceddia RB (2006) Regulation of AMP-activated protein kinase and acetyl-CoA carboxylase phosphorylation by palmitate in skeletal muscle cells. J Lipid Res 47:412–420. https://doi.org/10.1194/jlr.M500438-JLR200
Forrest LR, Krämer R, Ziegler C (2011) The structural basis of secondary active transport mechanisms. Biochim Biophys Acta - Bioenerg 1807:167–188. https://doi.org/10.1016/j.bbabio.2010.10.014
Fromm MF (2004) Importance of P-glycoprotein at blood–tissue barriers. Trends Pharmacol Sci 25:423–429. https://doi.org/10.1016/j.tips.2004.06.002
Garcia GE, Campbell AJ, Olson J, et al (2010) Novel oximes as blood-brain barrier penetrating cholinesterase reactivators. Chem Biol Interact 187:199–206. https://doi.org/10.1016/j.cbi.2010.02.033
Gašo Sokač D, Zandona A, Roca S, et al (2022) Potential of vitamin B6 dioxime analogues to act as cholinesterase ligands. Int J Mol Sci 23:13388. https://doi.org/10.3390/ijms232113388
Gaurav A, Gautam V (2014) Structure-based three-dimensional pharmacophores as an alternative to traditional methodologies. J Receptor Ligand Channel Res 27. https://doi.org/10.2147/JRLCR.S46845
Gunness P, Aleksa K, Kosuge K, et al (2010) Comparison of the novel HK-2 human renal proximal tubular cell line with the standard LLC-PK1 cell line in studying drug-induced nephrotoxicity. Can J Physiol Pharmacol 88:448–455. https://doi.org/10.1139/Y10-023
Handl J, Malinak D, Capek J, et al (2021) Effects of Charged Oxime Reactivators on the HK-2 Cell Line in Renal Toxicity Screening. Chem Res Toxicol 34:699–703. https://doi.org/10.1021/acs.chemrestox.0c00489
Hasemann CA, Kurumbail RG, Boddupalli SS, et al (1995) Structure and function of cytochromes P450:a comparative analysis of three crystal structures. Structure 3:41–62. https://doi.org/10.1016/S0969-2126(01)00134-4
Hengartner MO (2000) The biochemistry of apoptosis. Nature 407:145–153
Hepnarova V, Muckova L, Ring A, et al (2019) Pharmacological and toxicological in vitro and in vivo effect of higher doses of oxime reactivators. Toxicol Appl Pharmacol 383:114776. https://doi.org/10.1016/j.taap.2019.114776
Hewitt NJ, Hewitt P (2004) Phase I and II enzyme characterization of two sources of HepG2 cell lines. Xenobiotica 34:243–256. https://doi.org/10.1080/00498250310001657568
Jiménez E, Montiel M (2005) Activation of MAP kinase by muscarinic cholinergic receptors induces cell proliferation and protein synthesis in human breast cancer cells. J Cell Physiol 204:678–686. https://doi.org/10.1002/jcp.20326
Johnson DK, Karanicolas J (2016) Ultra-high-throughput structure-based virtual screening for small-molecule inhibitors of protein-protein interactions. J Chem Inf Model 56:399–411. https://doi.org/10.1021/acs.jcim.5b00572
Koichi Sakurada , Kazuo Matsubara, Keiko Shimizu, Hiroshi Shiono, Yasuo Seto, Koichiro Tsuge, Mineo Yoshino, Ikuko Sakai, Harutaka Mukoyama TT (2003) Pralidoxime iodide (2-pAM) penetrates across the blood-brain barrier. Neurochem Res 28:1401–7. https://doi.org/10.1023/a:1024960819430
König J, Müller F, Fromm MF (2013) Transporters and drug-drug interactions: Important determinants of drug disposition and effects. Pharmacol Rev 65:944–966. https://doi.org/10.1124/pr.113.007518
Kotake Y, Sekiya Y, Okuda K, Ohta S (2007) Cytotoxicity of 17 tetrahydroisoquinoline derivatives in SH-SY5Y human neuroblastoma cells is related to mitochondrial NADH–ubiquinone oxidoreductase inhibition. Neurotoxicology 28:27–32. https://doi.org/10.1016/j.neuro.2006.06.002
Kovalevich J, Langford D (2013) Considerations for the Use of SH - SY5Y Neuroblastoma Cells in Neurobiology. In: Neuronal Cell Culture: Methods and Protocols. pp 9–21
Kryston TB, Georgiev AB, Pissis P, Georgakilas AG (2011) Role of oxidative stress and DNA damage in human

carcinogenesis. Mutat Res - Fundam Mol Mech Mutagen 711:193–201. https://doi.org/10.1016/j.mrfmmm.2010.12.016
Li P, Zhou L, Zhao T, et al (2017) Caspase-9: Structure, mechanisms and clinical application. Oncotarget 8:23996–24008. https://doi.org/10.18632/oncotarget.15098
Lock EA, Reed CJ (1998) Xenobiotic metabolizing enzymes of the kidney. Toxicol Pathol 26:18–25. https://doi.org/10.1177/019262339802600102
Lorke D, Kalasz H, Petroianu G, Tekes K (2008) Entry of oximes into the brain: A review. Curr Med Chem 15:743–753. https://doi.org/10.2174/092986708783955563
Ma J, Qin L, Li X (2020) Role of STAT3 signaling pathway in breast cancer. Cell Commun Signal 18:33. https://doi.org/10.1186/s12964-020-0527-z
Mandel LJ (1986) Primary active sodium transport, oxygen consumption, and ATP: Coupling and regulation. Kidney Int 29:3–9. https://doi.org/10.1038/ki.1986.2
Matsson P, Kihlberg J (2017) How Big Is Too Big for Cell Permeability? J Med Chem 60:1662–1664. https://doi.org/10.1021/acs.jmedchem.7b00237
Mosmann T (1983) Rapid colorimetric assay for cellular growth and survival: application to proliferation and cytotoxicity assays. J Immunol Methods 65:55–63
Muckova L, Vanova N, Misik J, et al (2019) Oxidative stress induced by oxime reactivators of acetylcholinesterase in vitro. Toxicol Vitr 56:110–117. https://doi.org/10.1016/j.tiv.2019.01.013
OuYang B, Pochapsky SS, Dang M, Pochapsky TC (2008) A functional proline switch in cytochrome P450cam. Structure 16:916–923. https://doi.org/10.1016/j.str.2008.03.011
Pajouhesh H, Lenz GR (2005) Medicinal chemical properties of successful central nervous system drugs. NeuroRx 2:541–553
Pirkmajer S, Bezjak K, Matkovič U, et al (2020) Ouabain suppresses IL-6/STAT3 signaling and promotes cytokine secretion in cultured skeletal muscle cells. Front Physiol 11:. https://doi.org/10.3389/fphys.2020.566584
Polli JW, Wring SA, Humphreys JE, et al (2001) Rational use of in vitro P-glycoprotein assays in drug discovery. J Pharmacol Exp Ther 299:620–8
Ribeiro MMB, Castanho MAR., Serrano I (2010) In Vitro Blood-Brain Barrier Models – Latest Advances and Therapeutic Applications in a Chronological Perspective. Mini-Reviews Med Chem 10:263–271. https://doi.org/10.2174/138955710791185082
Roos WP, Kaina B (2006) DNA damage-induced cell death by apoptosis. Trends Mol Med 12:440–450. https://doi.org/10.1016/j.molmed.2006.07.007
Rosenberg YJ, Wang J, Ooms T, et al (2018) Post-exposure treatment with the oxime RS194B rapidly reactivates and reverses advanced symptoms of lethal inhaled paraoxon in macaques. Toxicol Lett 293:229–234. https://doi.org/10.1016/j.toxlet.2017.10.025
Roux PP, Blenis J (2004) ERK and p38 MAPK-activated protein kinases: a family of protein kinases with diverse biological functions. Microbiol Mol Biol Rev 68:320–44. https://doi.org/10.1128/MMBR.68.2.320–344.2004
Ryan MJ, Johnson G, Kirk J, et al (1994) HK-2: An immortalized proximal tubule epithelial cell line from normal adult human kidney. Kidney Int 45:48–57. https://doi.org/10.1038/ki.1994.6
Saggerson D (2008) Malonyl-CoA, a key signaling molecule in mammalian cells. Annu Rev Nutr 28:253–272. https://doi.org/10.1146/annurev.nutr.28.061807.155434
Saitoh T, Abe K, Ishikawa M, et al (2006) Synthesis and in vitro cytotoxicity of 1,2,3,4-tetrahydroisoquinoline derivatives. Eur J Med Chem 41:241–252. https://doi.org/10.1016/j.ejmech.2005.11.003
Sit RK, Kovarik Z, Maček Hrvat N, et al (2018) Pharmacology, pharmacokinetics, and tissue disposition of zwitterionic hydroxyiminoacetamido alkylamines as reactivating antidotes for organophosphate exposure. J Pharmacol Exp Ther 367:363–372. https://doi.org/10.1124/jpet.118.249383
Soukup O, Jun D, Tobin G, Kuca K (2013) The summary on non-reactivation cholinergic properties of oxime reactivators: The interaction with muscarinic and nicotinic receptors. Arch Toxicol 87:711–719. https://doi.org/10.1007/s00204-012-0977-1
Soukup O, Krušek J, Kaniaková M, et al (2011) Oxime reactivators and their in vivo and in vitro effects on nicotinic receptors. Physiol Res 60:679–686
Suzuki I, Kondoh M, Nagashima F, et al (2004) A comparison of apoptosis and necrosis induced by ent-kaurene-type diterpenoids in HL-60 cells. Planta Med 70:401–406. https://doi.org/10.1055/s-2004-818966
Sychev D, Ashraf GM, Svistunov A, et al (2018) The cytochrome P450 isoenzyme and some new opportunities for the prediction of negative drug interaction in vivo. Drug Des Devel Ther Volume 12:1147–1156. https://doi.org/10.2147/DDDT.S149069
Taylor P, Yan-Jye S, Momper J, et al (2019) Assessment of ionizable, zwitterionic oximes as reactivating antidotal

agents for organophosphate exposure. Chem Biol Interact 308:194–197. https://doi.org/10.1016/j.cbi.2019.05.015

Thomas P, Smart TG (2005) HEK293 cell line: A vehicle for the expression of recombinant proteins. J Pharmacol Toxicol Methods 51:187–200. https://doi.org/10.1016/j.vascn.2004.08.014

Timbrell JA (2000) Principles of Biochemical Toxicology, Third Edit

Truax VM, Zhao H, Katzman BM, et al (2013) Discovery of Tetrahydroisoquinoline-Based CXCR4 Antagonists. ACS Med Chem Lett 4:1025–1030. https://doi.org/10.1021/ml400183q

Tummers B, Green DR (2017) Caspase-8: regulating life and death. Immunol Rev 277:76–89. https://doi.org/10.1111/imr.12541

Van Quickelberghe E, De Sutter D, van Loo G, et al (2018) A protein-protein interaction map of the TNF-induced NF-κB signal transduction pathway. Sci Data 5:180289. https://doi.org/10.1038/sdata.2018.289

Worek F, Thiermann H (2013) The value of novel oximes for treatment of poisoning by organophosphorus compounds. Pharmacol Ther 139:249–259. https://doi.org/10.1016/j.pharmthera.2013.04.009

Worek F, Thiermann H, Wille T (2020) Organophosphorus compounds and oximes: a critical review. Arch Toxicol 94:2275–2292. https://doi.org/10.1007/s00204-020-02797-0

Wu Y, Zhao D, Zhuang J, et al (2016) Caspase-8 and Caspase-9 Functioned Differently at Different Stages of the Cyclic Stretch-Induced Apoptosis in Human Periodontal Ligament Cells. PLoS One 11:1–15. https://doi.org/10.1371/journal.pone.0168268

Xie HR, Hu L Sen, Li GY (2010) SH-SY5Y human neuroblastoma cell line: In vitro cell model of dopaminergic neurons in Parkinson's disease. Chin Med J (Engl) 123:1086–1092. https://doi.org/10.3760/cma.j.issn.0366-6999.2010.08.021

Zandona A, Katalinić M, Šinko G, et al (2020) Targeting organophosphorus compounds poisoning by novel quinuclidine-3 oximes: development of butyrylcholinesterase-based bioscavengers. Arch Toxicol 94:3157–3171. https://doi.org/10.1007/s00204-020-02811-5

Zandona A, Maraković N, Mišetić P, et al (2021) Activation of (un)regulated cell death as a new perspective for bispyridinium and imidazolium oximes. Arch Toxicol 95:2737–2754. https://doi.org/10.1007/s00204-021-03098-w

Zandona A, Zorbaz T, Miš K, et al (2022) Cytotoxicity-related effects of imidazolium and chlorinated bispyridinium oximes in SH-SY5Y cells. Arh Hig Rada Toksikol 73:277–284. https://doi.org/10.2478/aiht-2022-73-3688

Zorbaz T, Braïki A, Maraković N, et al (2018) Potent 3-hydroxy-2-pyridine aldoxime reactivators of organophosphate-inhibited cholinesterases with predicted blood–brain barrier penetration. Chem - A Eur J 24:9675–9691. https://doi.org/10.1002/chem.201801394

Zorbaz T, Mišetić P, Probst N, et al (2020) Pharmacokinetic evaluation of brain penetrating morpholine-3-hydroxy-2-pyridine oxime as an antidote for nerve agent poisoning. ACS Chem Neurosci 11:1072–1084. https://doi.org/10.1021/acschemneuro.0c00032

Zou M, Xia S, Zhuang L, et al (2013) Knockdown of the Bcl-2 gene increases sensitivity to EGFR tyrosine kinase inhibitors in the H1975 lung cancer cell line harboring T790M mutation. Int J Oncol 42:2094–2102. https://doi.org/10.3892/ijo.2013.1895